

Airborne Microbial Decontamination using Dielectric Barrier Discharge Technology - Phase II

Study Report

(2015-2016)

Submitted to Novaerus Inc.,

Dr. Ram Prasad Gandhiraman,

Principal Investigator

Universities Space Research Association

615 National Avenue, Suite 220

Mountain View, CA 94043

Email: ramprasad.gandhiraman@nasa.gov

Ms. Jaione Romero-Mangado,

Microbiologist

Science & Technology Corporation

NASA Ames Research Center

N239 R175

Moffett Field, CA 94035

Phone: 650-604-0323

Email: jaione.romeromangado@nasa.gov

Oct 17, 2016

Aim

The objective of the research is to explore the efficacy of dielectric barrier discharge (DBD) technology for deactivating airborne micro-organisms and study the effects of the DBD on surface chemistry and morphology of aerosolized *Staphylococcus epidermidis*.

Researchers, Advisors and Collaborators who provided valuable scientific comments

Ms. Jaione Romero-Mangado,

Microbiologist
Science & Technology Corporation
NASA Ames Research Center
N239 R175
Moffett Field, CA 94035
Phone: 650-604-0323
Email: jaione.romeromangado@nasa.gov

Dr. Dennis Nordlund,

Staff Scientist,
SLAC National Accelerator Laboratory,
Menlo Park, CA-94025
Email: nordlund@slac.stanford.edu

Ms. Diana C. Diaz-Cartagena,

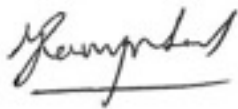
Department of Chemistry,
University of Puerto Rico,
Río Piedras Campus, San Juan, P.R. 00931

Ms. Nadja E. Solis-Marcano,
Department of Chemistry,
University of Puerto Rico,
Río Piedras Campus, San Juan, P.R. 00931

Mr. Avishek Dey
Visiting Research Scholar,
NASA Ames Research Center
Moffett Field, California 94035, USA
&
Research Student,
Materials Engineering
The Open University
Milton Keynes, UK
Email: avishek.dey@nasa.gov

Electron Microscopy study:

The scanning electron microscopy study was performed at UCSC Materials Analysis for Collaborative Science (MACS) user Facility, an advanced microscopy and materials facility, located at NASA Ames Research Center in Mountain View, CA.



Dr. Ram Prasad Gandhiraman
Principal Investigator,
Universities Space Research Association,
NASA Ames Research Center,
Mountain View, California.
Email: rgandhiraman@usra.edu; ramprasad.gandhiraman@nasa.gov

TABLE OF CONTENTS

ABSTRACT.....	5
INTRODUCTION.....	6
EXPERIMENTAL WORK.....	8
RESULTS.....	13
X-RAY ABSORPTION SPECTROSCOPY OF S. EPIDERMIDIS	32
ASPERGILLUS NIGER.....	36
CONCLUSIONS.....	42
REFERENCES.....	43

Airborne Microbial Decontamination using Dielectric Barrier Discharge Technology: *Staphylococcus epidermidis* & *Aspergillus niger*

ABSTRACT

Atmospheric pressure plasma technology has gained increased attention in the recent past for several environmental applications. This technology could potentially be used to deactivate airborne microbes and surface bound microbes and biofilms. In this work, we explore the efficacy of the atmospheric pressure dielectric barrier discharge (DBD) technology for inactivating airborne pathogens. *Staphylococcus epidermidis* is an opportunistic pathogen known to cause nosocomial infection.¹ In order to understand the effect of DBD on the cell structure, we study the effect of DBD on the morphology of aerosolized *Staphylococcus epidermidis* using Scanning Electron Microscopy (SEM). The images obtained from this surface analysis technique showed that the bacteria underwent severe physical deformation, possibly causing effective inactivation of *S. epidermidis*. Severe damage to the cell structure upon interaction with the DBD possibly resulting in leakage of vital cellular materials might be one of the key mechanisms for inactivation of *S. epidermidis*. Also, surface chemical change of the microbes upon interaction with the short-lived reactive oxygen species from the DBD might also be contributing towards bacterial inactivation. Thus, the chemical structure of the microbial cell surface was analyzed by x-ray absorption spectroscopy before and after DBD exposure. Inactivation of Fungal spores of *Aspergillus niger* was also carried out to prove the versatility of the equipment.

1. INTRODUCTION

Staphylococcus epidermidis is a gram-positive bacterium that colonizes the human epithelium. *S. epidermidis* emerges as an opportunistic pathogen and a common cause for nosocomial infections leading to chronic infections.^{2,3} These bacteria are known to form biofilms on medical implants and catheters.⁴⁻⁶ *S. epidermidis*, a coagulase-negative *Staphylococcus* is a leading cause of infection in immunocompromised, long-term hospitalized and critically ill patients.^{7,8} Atmospheric pressure plasmas have been researched as an alternative and a robust approach for sterilization of surfaces, medical devices and surgical tools.⁹⁻¹¹ The efficiency of different types of tools vary according to the nature and type of plasma generation, gas mixtures, flow rates, gas temperature and treatment area.^{12,13} To the best of our knowledge, there has not been much work done on the application of atmospheric plasmas for inactivation of air borne pathogens. Dielectric barrier discharge is a type of atmospheric plasma that we employ for deactivation of air borne pathogens.

This study focuses on exploring the efficacy of dielectric barrier discharge technology for deactivating airborne microorganisms and to study the effects of the atmospheric pressure plasma on gram-positive bacteria. Previous research using a DBD system from Novaerus, have been conducted using *Escherichia coli*, a gram-negative microorganism. The physical and chemical changes on the air borne *E. coli* upon treatment with DBD were studied in detail.¹⁴ It was concluded that *E. coli* cell structure was damaged to varying extent as well as severe oxidation of the

cell membrane proving effective inactivation of the bacteria. In this study, gram-positive *S. epidermidis* is aerosolized and the effect of DBD is studied in detail.

The mechanisms of bacterial deactivation are well established and plenty of literature is available. Similarly, a vast number of literature is available on the sterilization effect of atmospheric pressure helium/argon/oxygen plasmas on surface bound bacteria.¹⁵⁻¹⁷ Few groups have studied the effect of atmospheric pressure plasmas that uses helium or argon gas as a primary plasma source, on surface bound *S. epidermidis*.¹⁸ We would like to highlight the fact that this study is on the effect of air based dielectric barrier discharge (with no additional gas supply) on air borne bacteria and provides a detailed spectroscopic analysis of the impact of DBD on aerosolized *S. epidermidis*. DBD for air borne microbial inactivation is a radically new approach in exploring the use of atmospheric pressure plasmas for environmental applications by eliminating any gas cylinder requirement and by developing a process that can run continuously for 24×7 without any manual interference for deactivating air borne microbes. The focus of this article is to study the ability of the DBD to inactivate air borne *Staphylococcus epidermidis* and to study its morphological and chemical changes upon treatment. Further study with relevant microbes could prove this technology to be a possible alternative approach to air hygiene. *Staphylococcus epidermidis* nebulized in air was exposed to the DBD and the bacterial sample collected from air was examined for detailed analysis.

2. EXPERIMENTAL WORK

Materials:

Staphylococcus epidermidis (*S. epidermidis*) (Migula) Castellani and Chalmers (ATCC 25922) was rehydrated in 1 ml of Tryptic soy Broth (BD 211825). The aliquot was aseptically transferred into a tube containing 10 ml of Tryptic Soy Broth and incubated overnight with shaking at 37. The cell culture was used for the experiment.

Spore preparation:

Aspergillus niger (ATCC 15475) was inoculated in sterile distilled water and incubated overnight at room temperature for propagation. *A. niger* spores were harvested aseptically in potato dextrose agar (Becton Dickinson 213400) and incubated for 5 days at 24. Individual spores were then isolated to conduct DBD studies. The spores were also placed on previously sterilized bare silicon wafers for scanning electron microscope imaging.

Experimental setup:

A compressor nebulizer was used to aerosolize spores into the DBD system (NV200, Novaerus Inc.) for sterilization testing. The DBD system used for this purpose consisted of two coaxial cylindrical coils made from stainless steel (AISI:304) wires of 0.2 mm diameter. The coils were separated by a borosilicate glass tube which acted as the dielectric barrier. The Dimensions of the glass tube being length = 80 mm, internal diameter = 22.5 mm, and outer diameter = 28 mm. The

spores were nebulized using OMROM Compressor nebulizer model NE-C29-E and the entire setup was kept inside a Bio-Safety Cabinet (Nuair, Class II, Type A2, Model NU-425-400). A high alternating voltage (4 kV) was applied between the electrodes to create the plasma discharge. The DBD system was equipped with a fan to draw the aerosolized output of nebulizer. All the DBD system vents except the top one were sealed to prevent any undesired micro-organism from getting into the system. The fungal suspension containing *A. niger* spores and distilled water of quantity 1 ml was transferred to the compressor nebulizer. The aerosolized particles were then fed through the top input and any viable particles after DBD treatment were collected at the output on sterile silicon wafers.

SEM characterization:

A Hitachi S4800 scanning electron microscope (SEM) was used to see the morphology of the spores before and after exposure to DBD. Aerosolized spores were first deposited in previously sterilized 1cm×1cm bare silicon wafers. The spores were then fixed in a 2.5% Glutaraldehyde solution in phosphate buffered saline during 2 hours. After the first fixation procedure the samples were rinsed with phosphate buffered saline and then, a 1% Osmium tetroxide solution in phosphate buffered saline was used as a second fixative process for 1 hour and 30 minutes. The samples were then dehydrated in gradually increasing concentrations of ethyl alcohol ranging from 60% to 100% for 50 minutes and exposed to hexamethyldisilazane for 5 minutes.

X-ray absorption spectroscopy (XAS):

XAS was also used to understand the changes in surface chemistry of bacteria. The near edge x ray absorption fine spectroscopy (NEXAFS) measurements were performed on beamline 8-2 (bending magnet endstation, spherical grating monochromator) at the Stanford Synchrotron Radiation Lightsource (SSRL).¹⁹ A gold grid in the beam path upstream of the chamber was used for the normalization of the incoming flux. The samples were mounted on an aluminum stick with carbon tape, and all the measurements were done under UHV conditions ($<1 \times 10^{-8}$ Torr) in a generic XPS/XAS chamber, equipped with a double pass cylindrical mirror analyzer (PHI 15-255 G) mounted perpendicular to the incoming beam axis in the horizontal plane. All measurements were performed at the magic angle ($\sim 55^\circ$ incidence), and the spectrometer detected electrons emitted along the e-vector of the incoming radiation (90° with respect to the incoming light in the horizontal plane). XAS data analysis was performed using Igor Pro. The bacterial samples collected on silicon wafer were freeze-dried using Labconco's Free Zone 4.5 Liter Freeze Dry Systems.

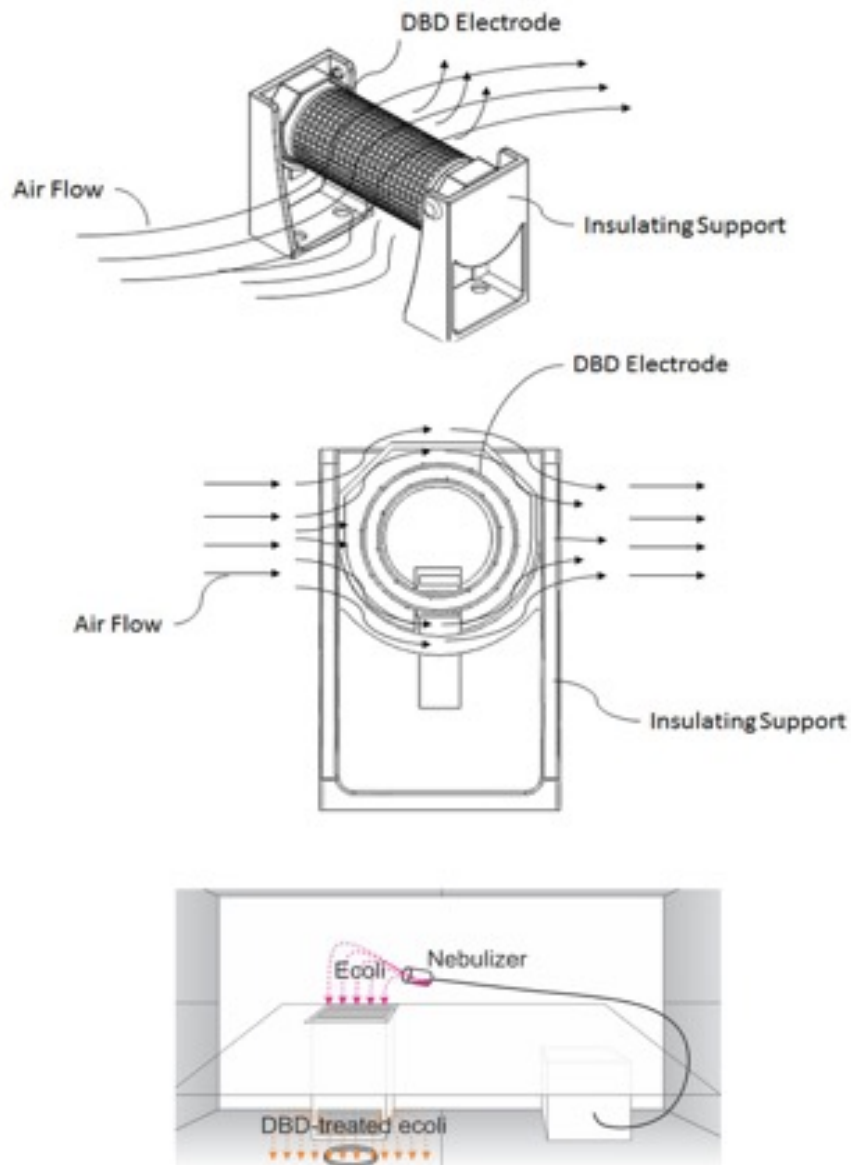


Figure 1. (a) Schematic of the NV200 DBD system showing the diagram of the assembled coil, (b) cross section illustrating the air flow around the dielectric barrier discharge, (c) the experimental setup for inactivation *E. coli* and sample collection

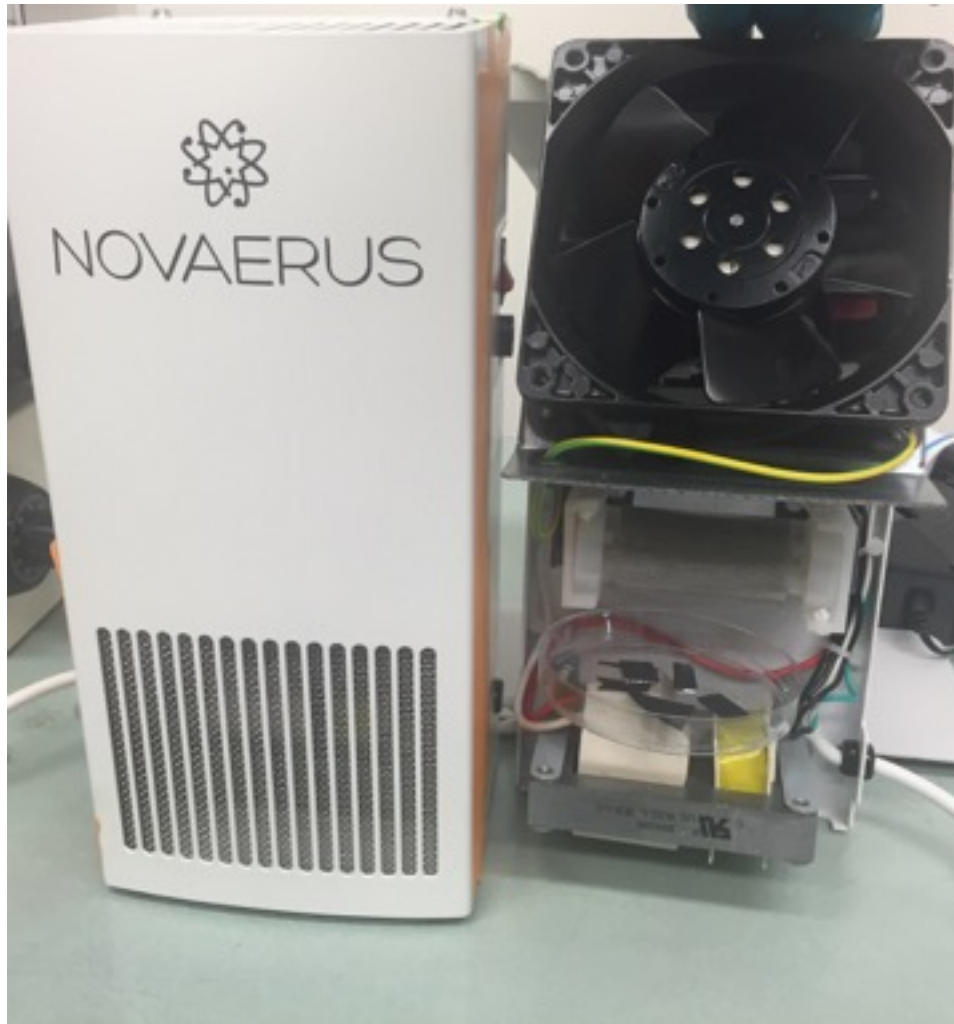
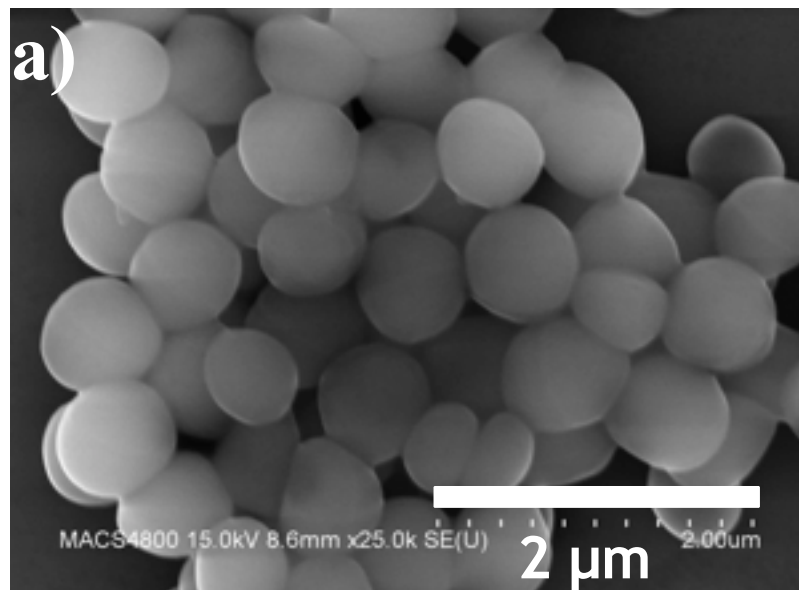


Figure 2. The photograph of the actual setup in the biosafety cabinet

3. RESULTS

1. Dropcasted *S. epidermidis* on Silicon wafer, without exposing to DBD

Staphylococcus epidermidis samples were dropcasted on silicon wafer, fixed using standard protocols and imaged under scanning electron microscopy. These images shows the size, shape and morphology of the untreated bacteria. From the SEM images it is very evident that the Staphylococcus epidermidis bacteria is less than 1 μ m diameter and the microorganism's size varies from 500nm to 1 μ m diameter. Also the micro organisms are spherical with no apparent structural damage in any of the SEM images.



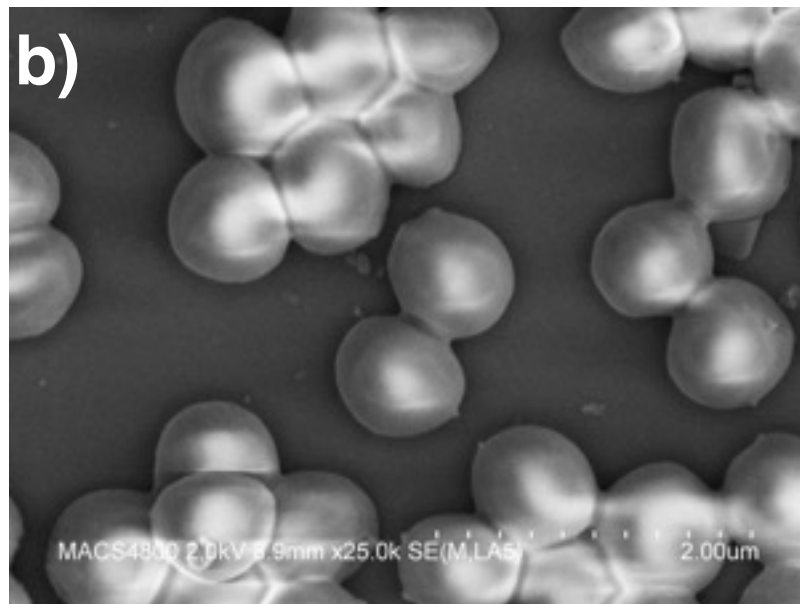
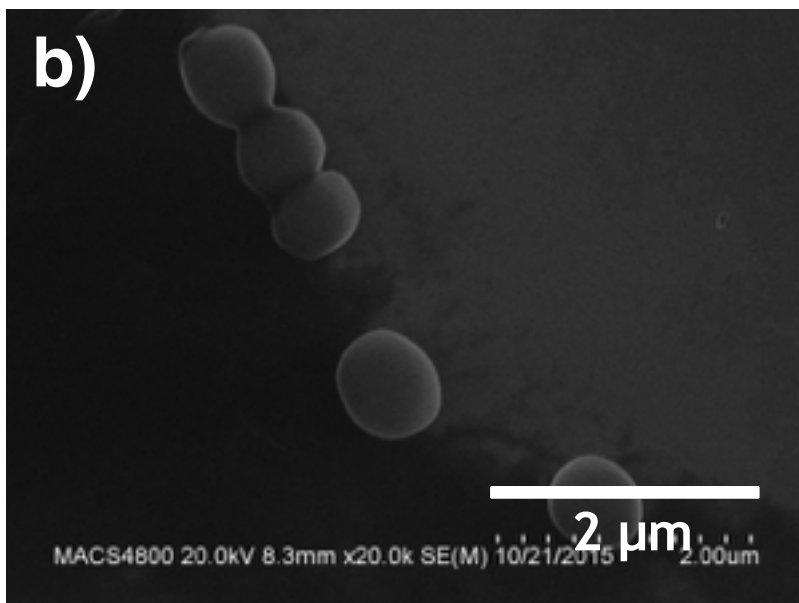
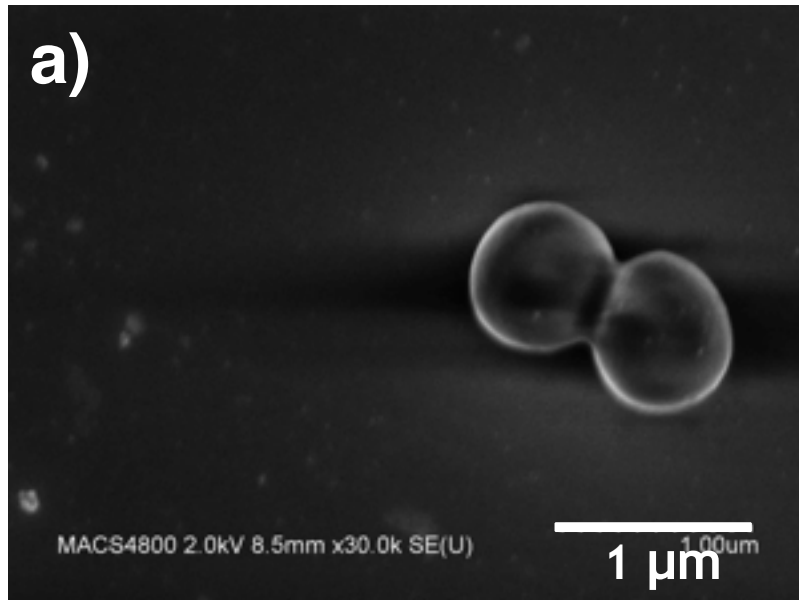


Figure 3. SEM images of drop casted *Staphylococcus epidermidis* on silicon wafer. a) and b) correspond to two sets of samples.

2. DBD and Fan OFF

As a control test, *Staphylococcus Epidermidis* was aerosolized and passed through the DBD system with both the fan and DBD turned off. It is observed that the bacteria retains its shape, size and morphology as shown in figures 4 a to d. Figures 4b and 4c shows that the bacteria are not completely isolated and some of them are clumped together. Figure 4d shows a single bacteria.



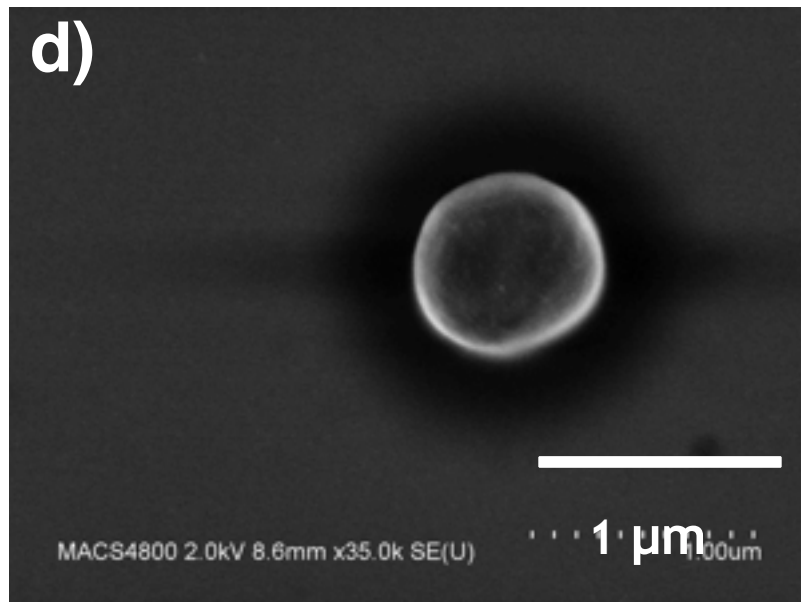
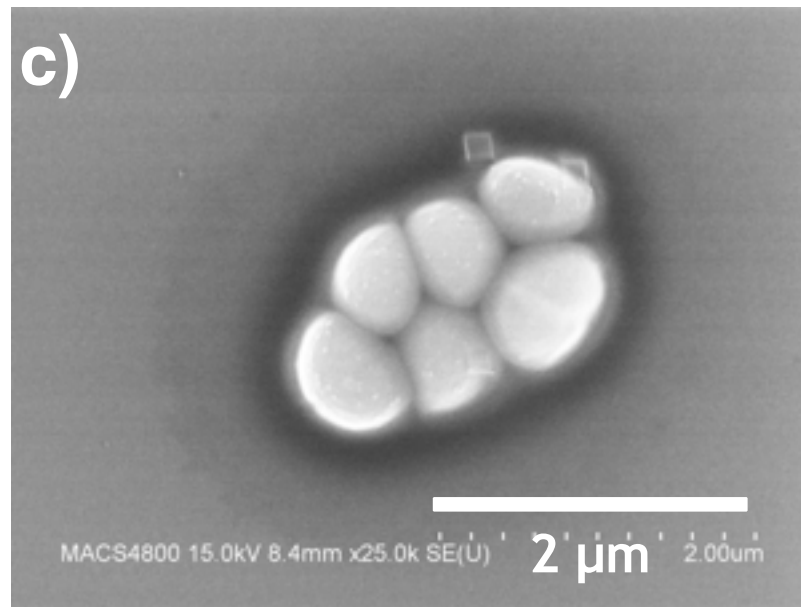
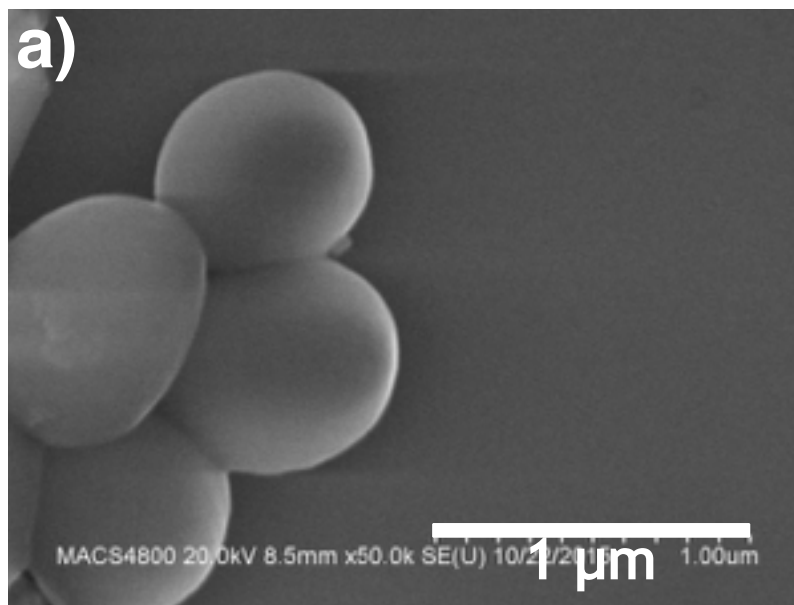
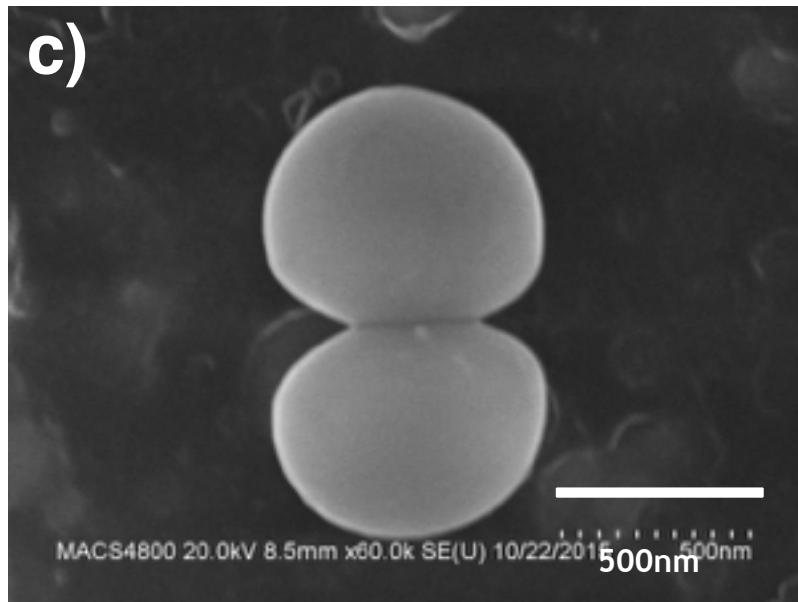
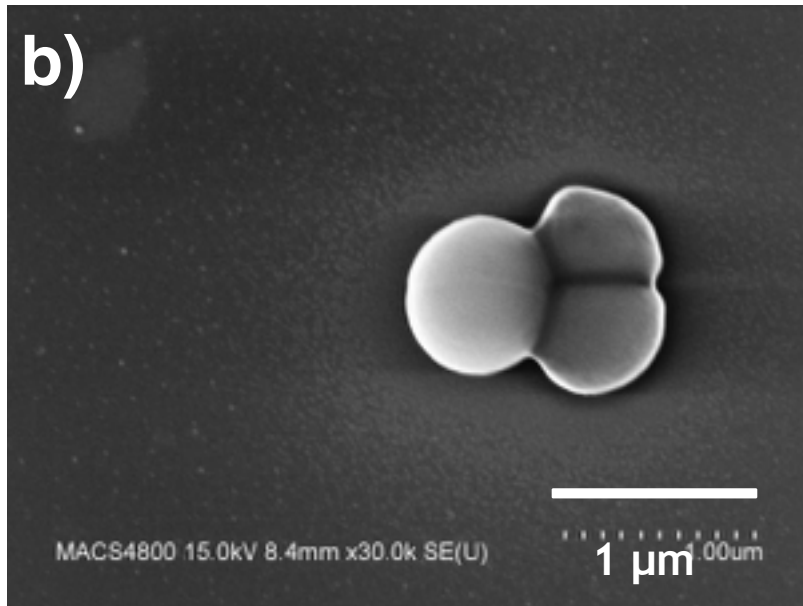


Figure 4. SEM image of *Staphylococcus Epidermidis*, aerosolized and collected in a silicon wafer with both DBD and Fan OFF.

3. Aerosolized, DBD OFF and Fan ON

The DBD units carry two controls, one for the fan that pulls the air towards the discharge and another for the electrodes that create the discharge. Another control experiment was performed with DBD turned off and fan turned on. The bacteria retains its shape, size and morphology. The purpose of this experiment is to use this as a control. When the actual inactivation process takes place, both the fan and the DBD should be turned on simultaneously. With the fan turned on the air borne microbes will be effectively pulled towards the discharge. In order to efficiently study the effect of DBD on the microbes, it is essential to perform a control experiment with fan turned on and with DBD off. It is observed from figures 5a to 5e that the control experiment with fan on and DBD off did not result in any significant change in the morphology of the microbes.





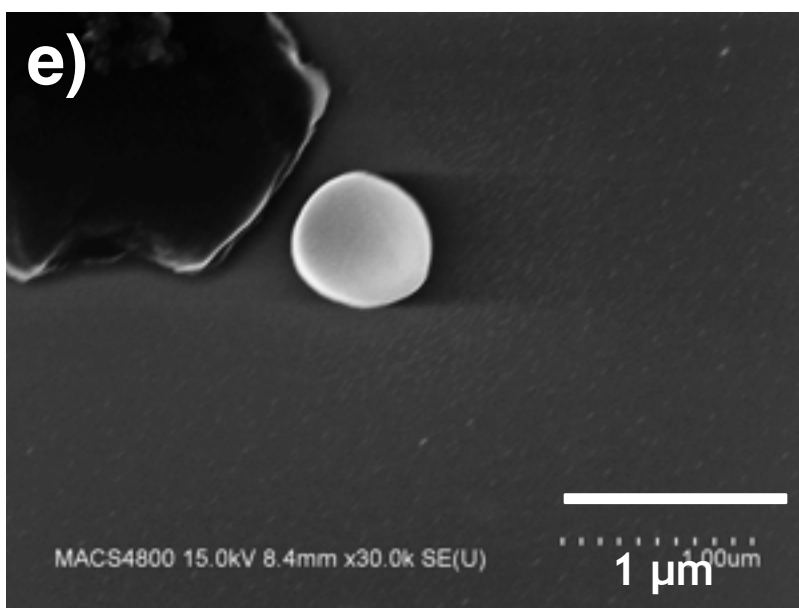
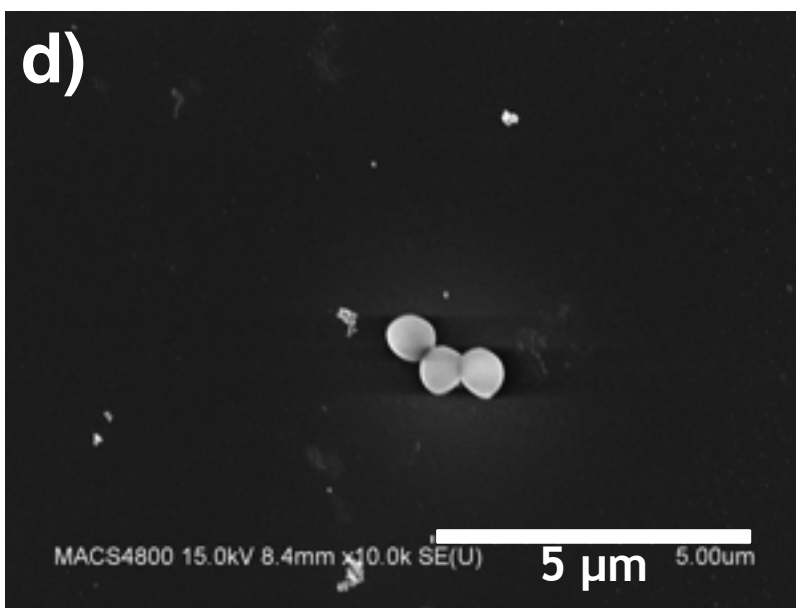
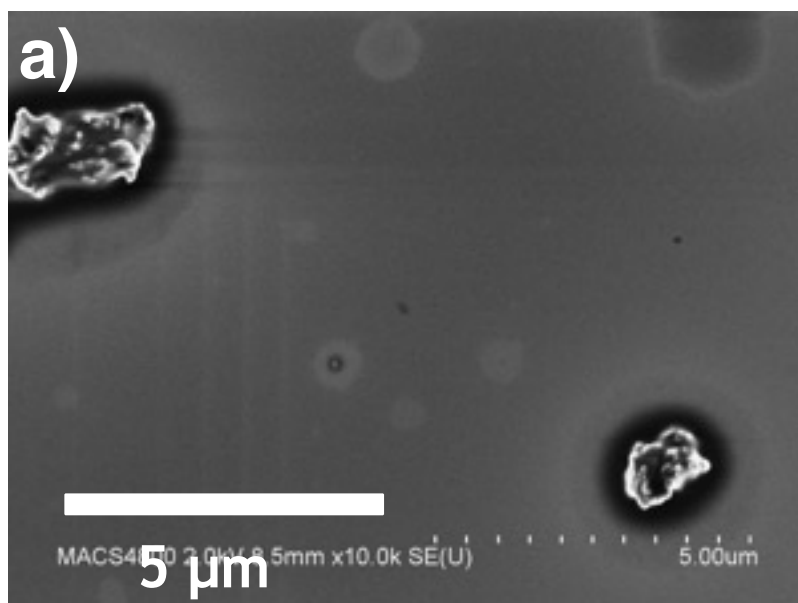
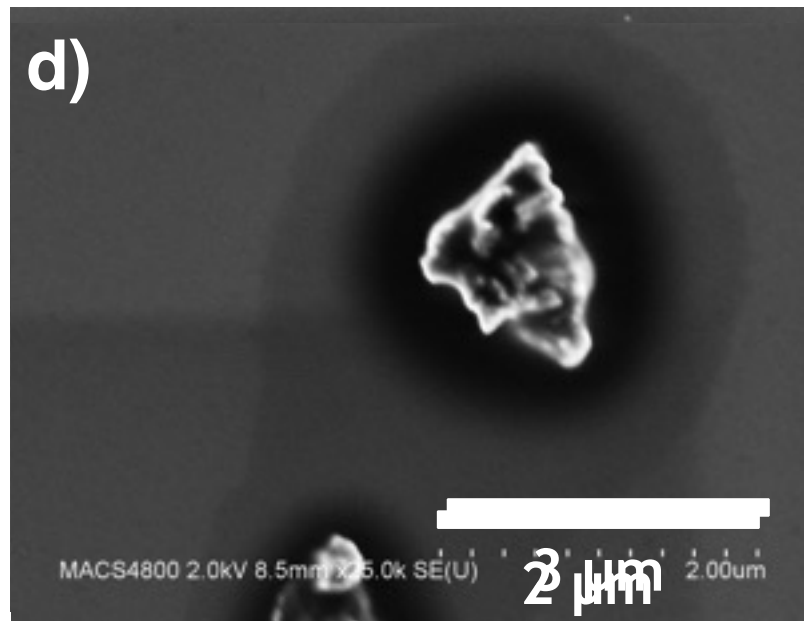
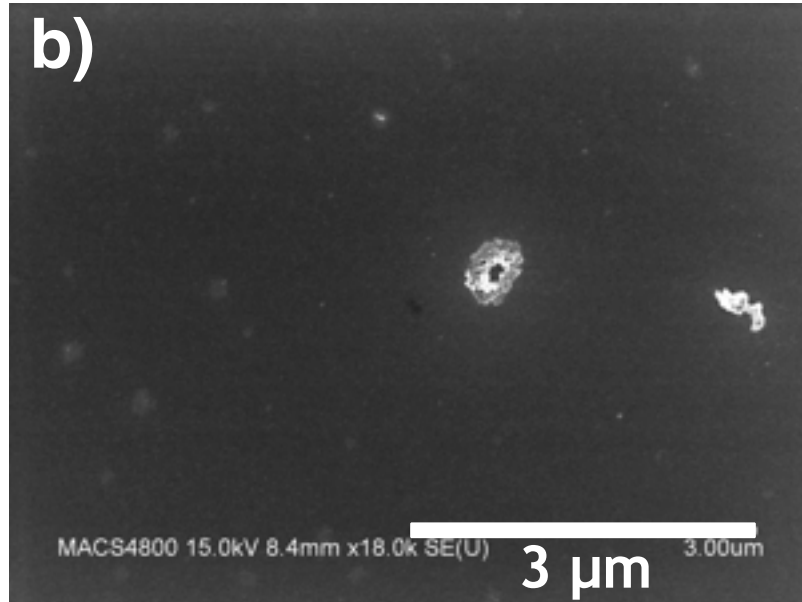


Figure 5. SEM images of *Staphylococcus epidermidis* aerosolized and captured on a silicon wafer with DBD OFF and Fan ON.

4. Aerosolized, DBD ON and Fan ON

Actual deactivation study with both DBD and Fan turned on. The SEM images shows that the bacteria undergoes severe structural damage, resulting in breakage of cell structure. It is clear from the below images that not all microbes undergo structural damage to the same extent. Figures 6a to 6e shows that the *staphylococcus epidermidis* has lost its spherical shape and the cell structure is damaged severely resulting in complete distortion of the cell structure. A similar behavior was also observed with *E. coli* measured during the phase 1 project. See Figure 4g in phase 1 report on *E. coli*. It is observed in Figure 4e that the three-dimensional structure of the microbe is also lost due to interaction with the DBD.





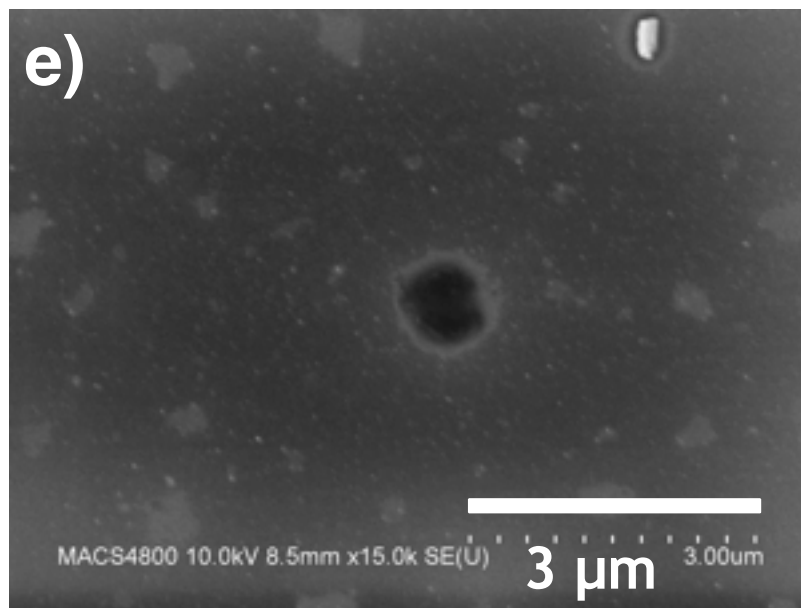
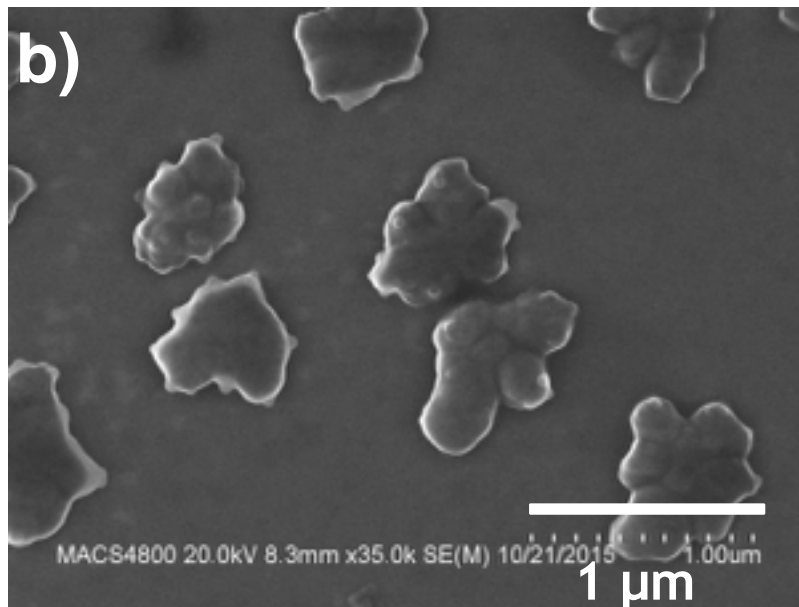
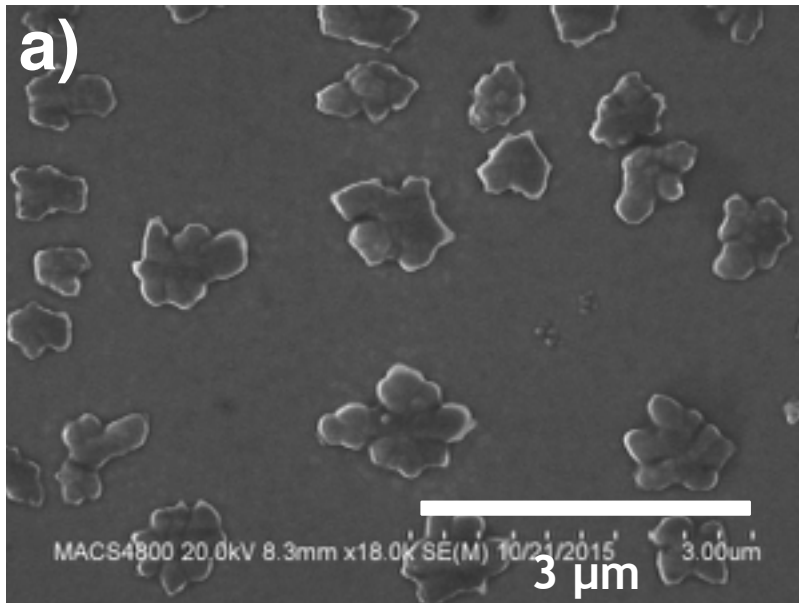
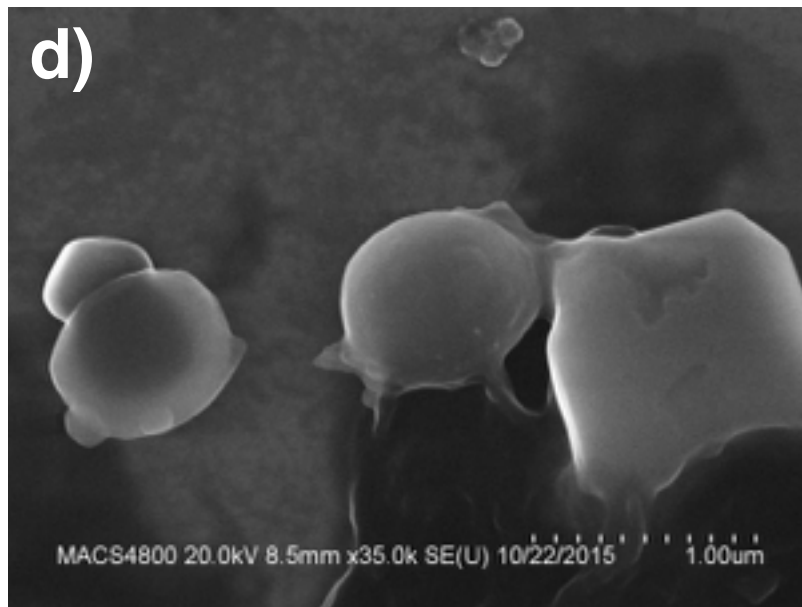
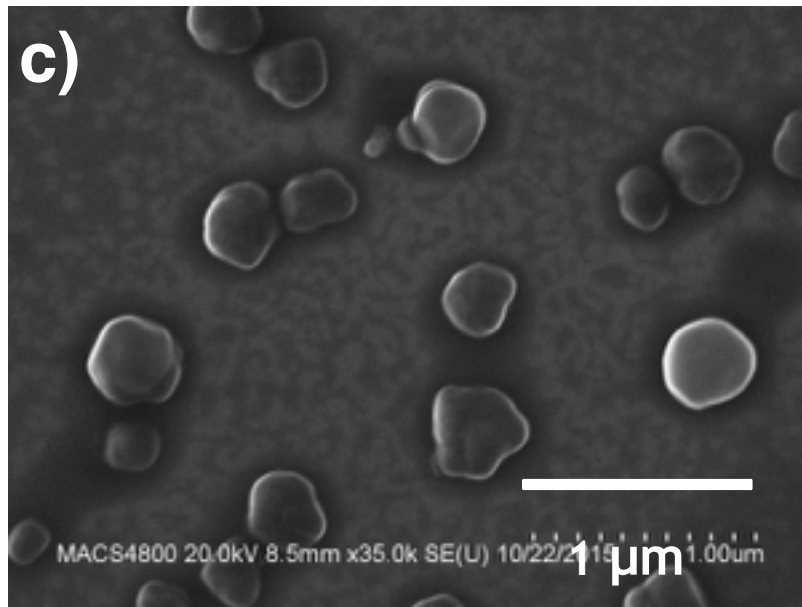


Figure 6. SEM images of *Staphylococcus epidermidis* aerosolized and captured on silicon wafer with both DBD and fan turned on.

Another set of *staphylococcus epidermidis* micro-organisms were aerosolized, passed through DBD system and captured on a silicon wafer placed in front of the outlet. The microbes were deformed uniformly with flattening of the edges. Figures 7a to 7d shows a clear flattening of the microbes with deformation of the cell structure. Unlike the figure 6, these set of microbes had different morphology after exposure to DBD but were deformed significantly probably resulting in loss of cellular materials. Figure 7d bottom right shows the flat edges in which part of the cellular materials are lost. Hence the three dimensional spherical structure is lost as is evident from the SEM images in figures 7a to 7d.





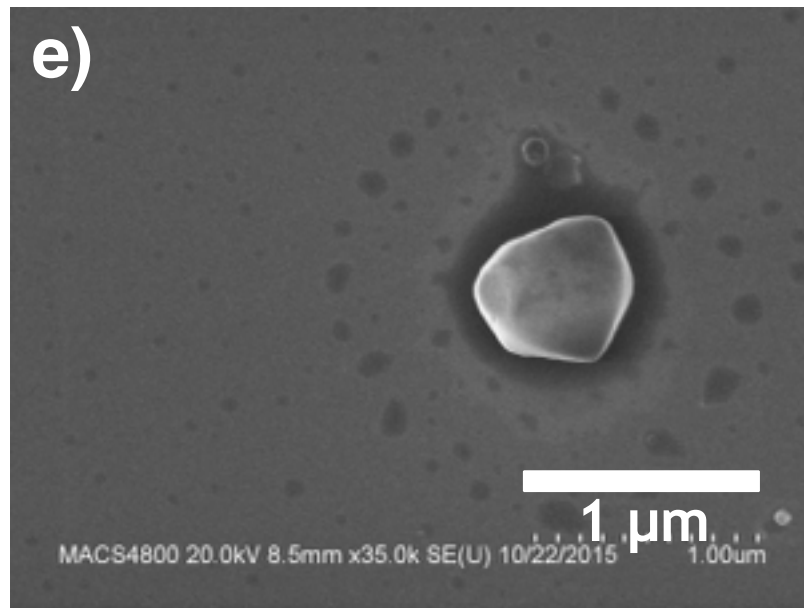
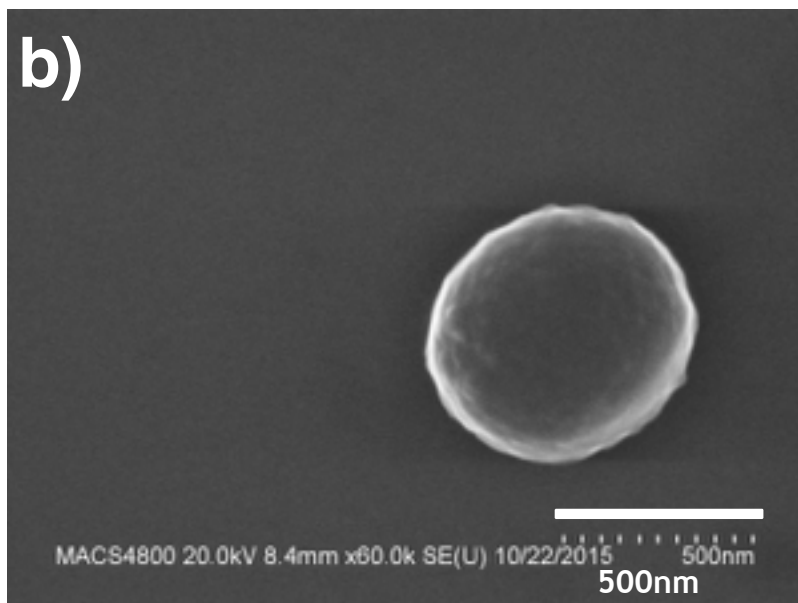
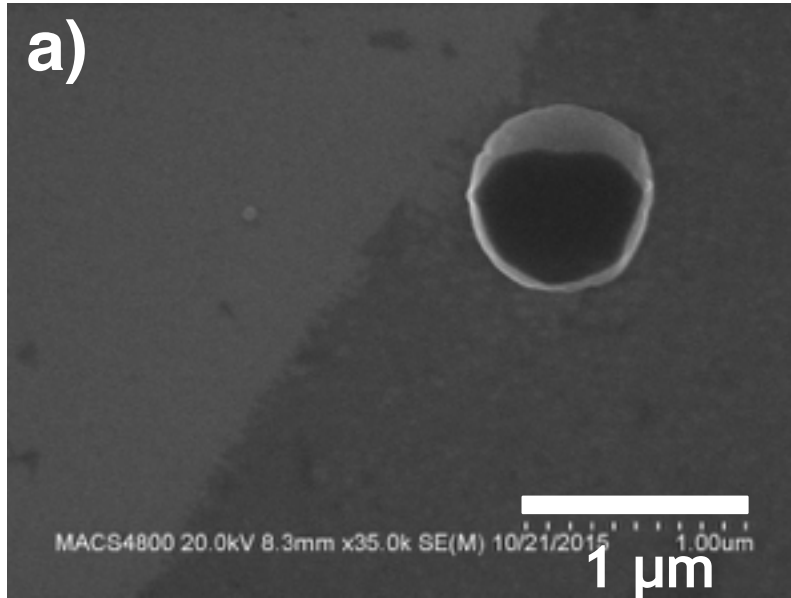


Figure 7. SEM images of *Staphylococcus epidermidis* aerosolized and captured on silicon wafer with both DBD and fan turned on.

In the actual deactivation measurement with both DBD and fan ON, the microbes collected on silicon wafer varied in their morphology, structure and shape significantly. There was no single pattern of structural deformation. A range of structural damage and deformation was observed. Also some of the microbes had retained their shape and size after the inactivation experiment with both DBD and Fan ON. It evidently points out to the fact that not all the microbes used in the study are affected and are inactivated. Part of the microbes retained their shape and size and were probably not affected.



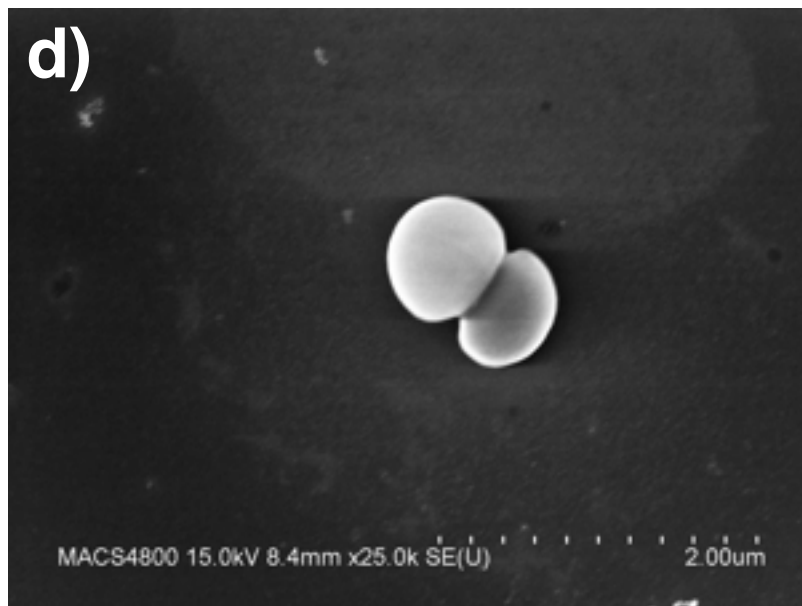
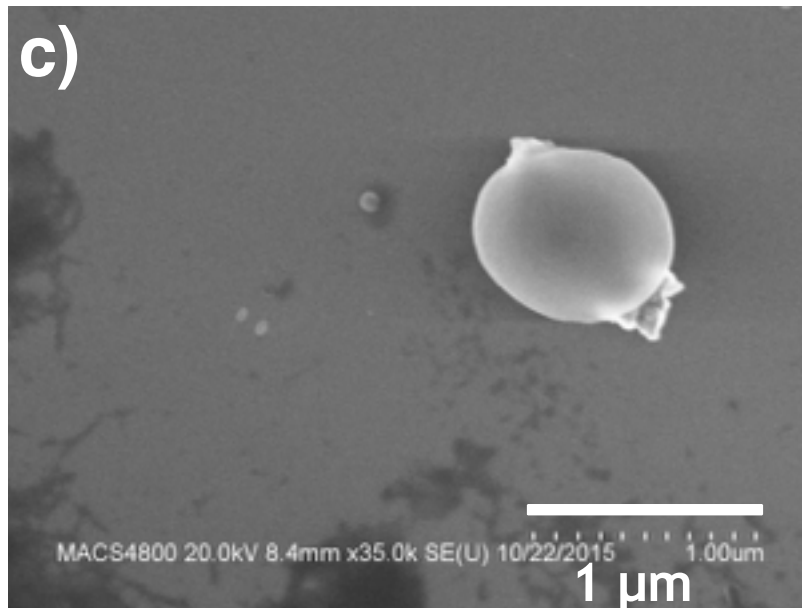


Figure 8. SEM images of *Staphylococcus epidermidis* aerosolized and captured on silicon wafer with both DBD and fan turned on.

5. Aerosolized DBD ON & Fan ON: Silicon wafer placed inside the DBD tool.

In this test, the samples were collected from inside the DBD system, with the front case open and silicon wafer placed right below the DBD coil. In the earlier experiments the silicon wafers were placed outside the DBD tool, right in front of the outlet. However, in this experiment the DBD tool case was opened and the silicon wafers were placed inside the DBD tool, right below the DBD coil and the tool case was closed during the measurement. The objective of this experiment is to eliminate settling of microbes that are not exposed to DBD. By placing a silicon wafer inside an enclosed DBD tool right below the electrodes, only the microbes that are passed through the DBD are collected.

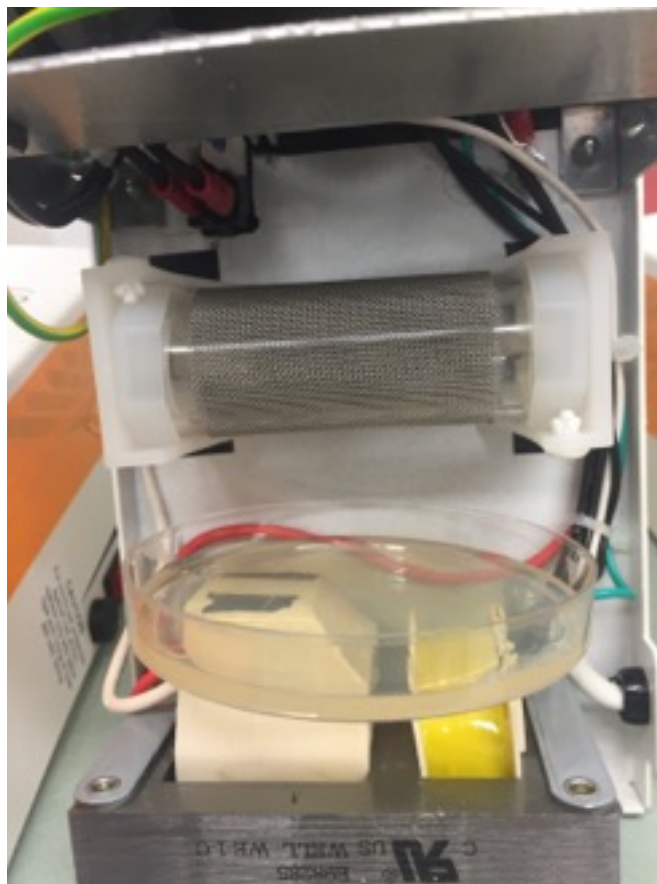
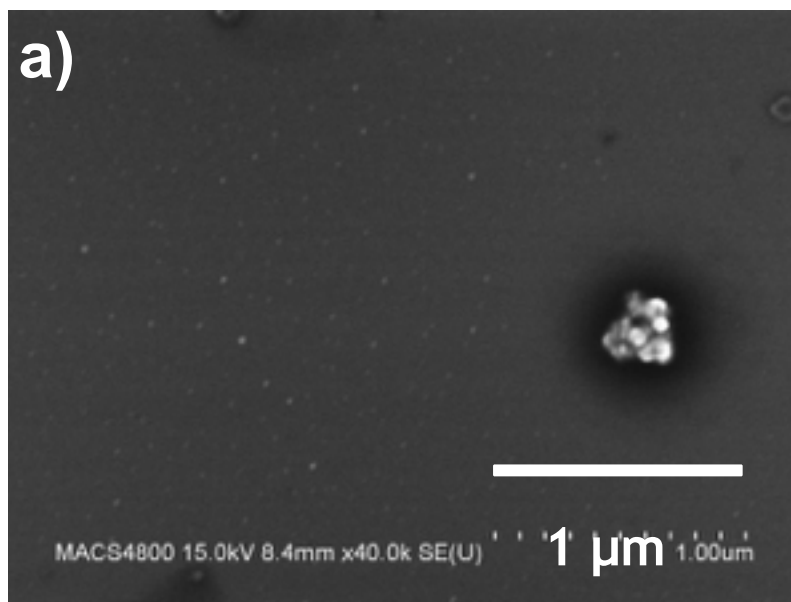
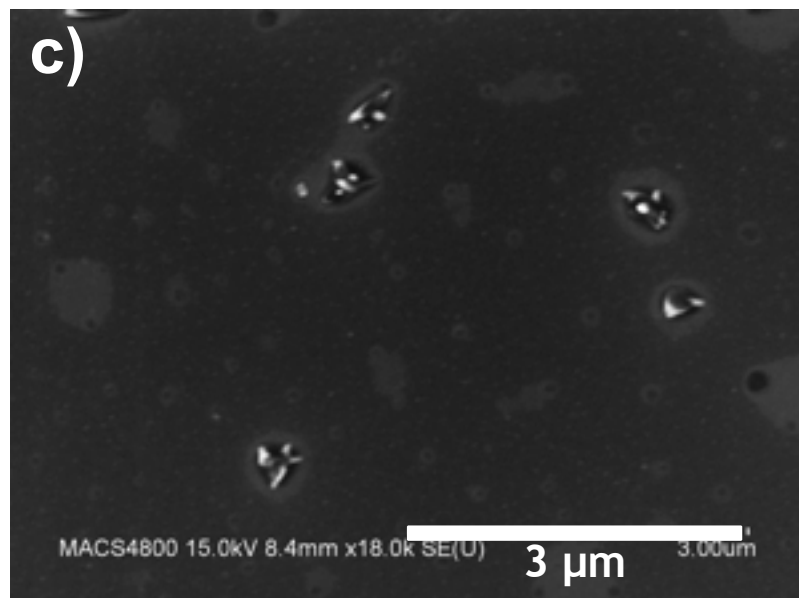
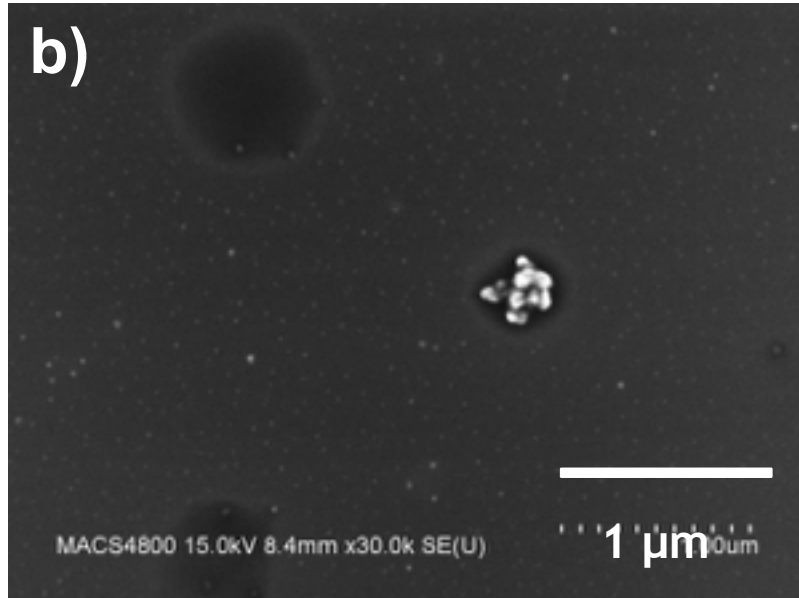


Figure 9. Photograph of the DBD tool with silicon wafer placed right below the electrodes.

Figure 10 shows the SEM images of staphylococcus epidermidis placed inside the DBD tool, under the electrodes with the case closed during the experiment. It is very evident that the microbes aerosolized and passed through the DBD undergo severe size and shape change possibly resulting in structural damage resulting in cell death. The size and shape change on all the samples are significantly high and in most of the cases the microbes are torn apart with loss of cellular materials.





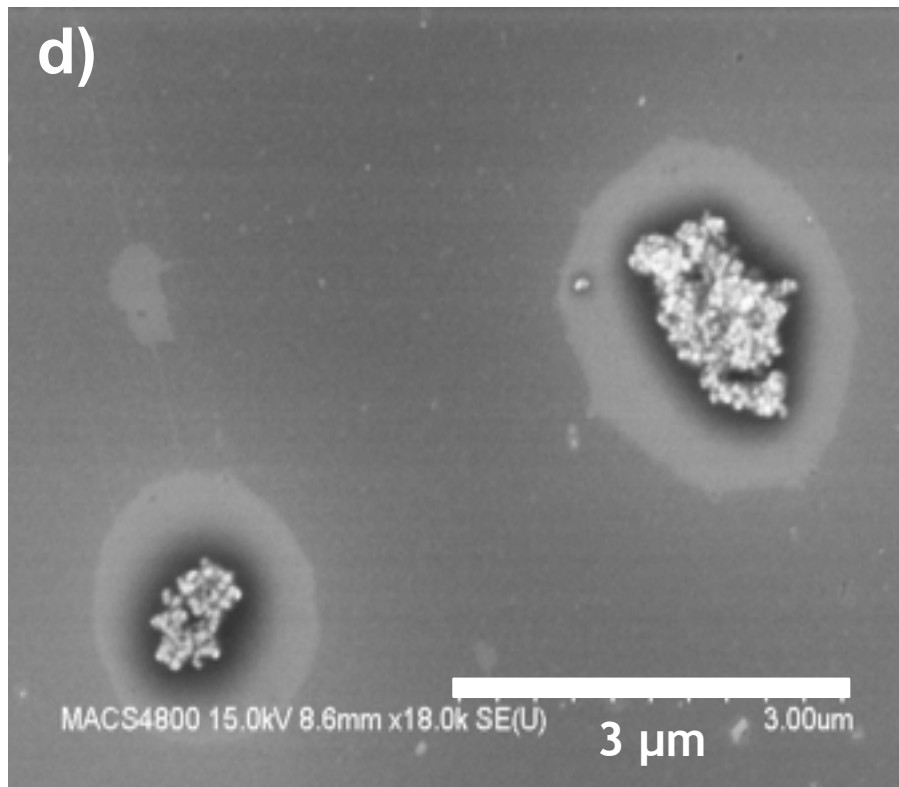
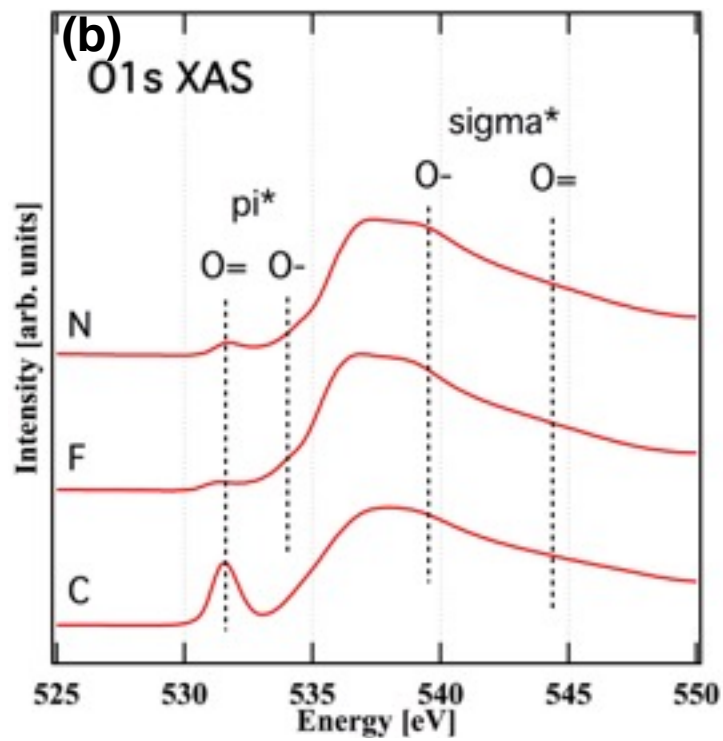
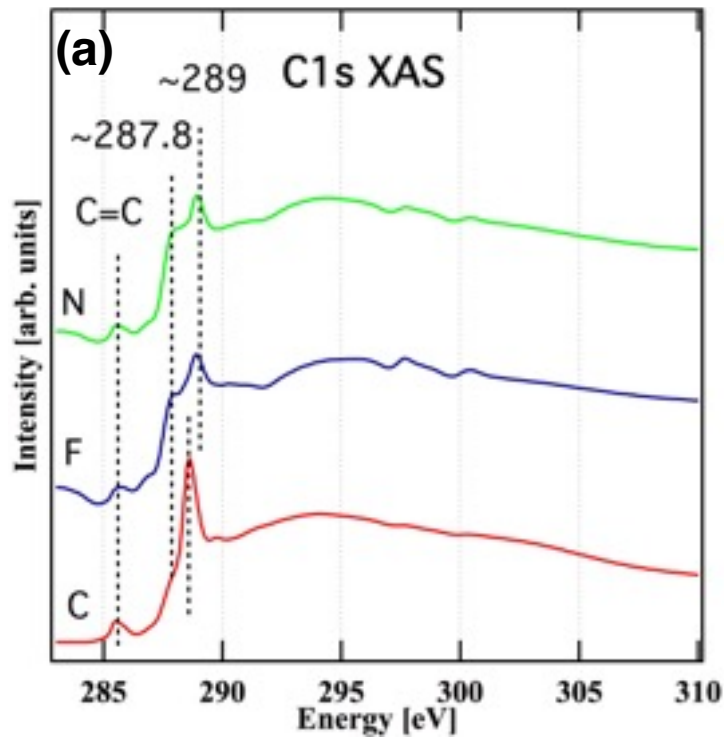


Figure 10. SEM images of staphylococcus epidermidis aerosolized and collected on silicon wafer placed inside the DBD tool, underneath the electrode.

4. X- RAY ABSORPTION SPECTROSCOPY



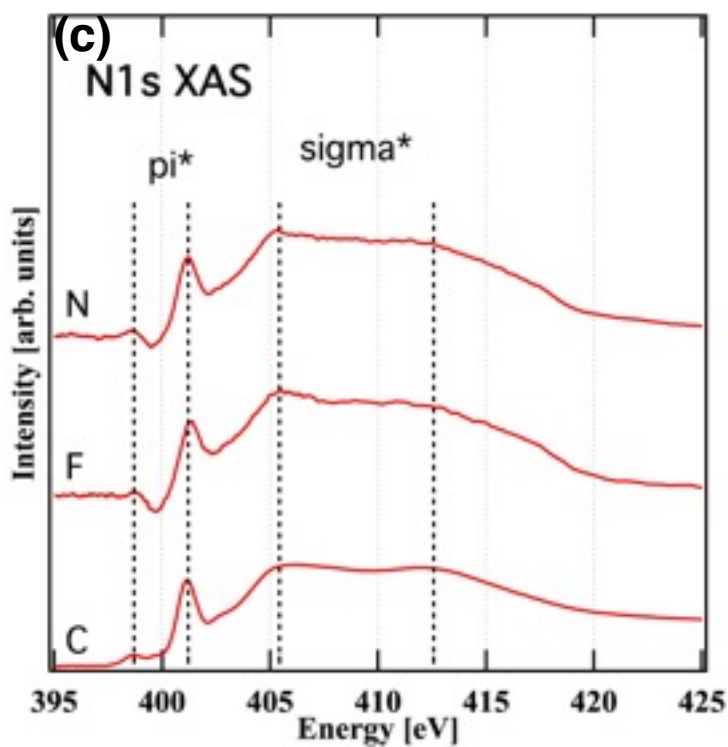


Figure 11. Core level X ray absorption edge of (a) Carbon K-edge (b) Oxygen K-edge (c) Nitrogen K edge. C corresponds to control sample, F corresponds to DBD off and Fan on, N corresponds to DBD on and Fan on.

Absorption spectra from each functionalized state has been presented in Figure 11. The spectra presented here presents a comparison between the surface functionalization of control with DBD off (D1) and on (D2) conditions. As fan had no evident effect on the bacteria morphology, so we kept the fan on for both the cases just to identify the changes in surface chemistry of the bacteria due to DBD. The peak at 285.5 eV in the carbon spectra [Figure 11 (a)] of all the samples correspond to π^* C=C transitions. The intensity drop at 285 eV may be due to the effect of normalization of the spectra as it matches with carbon dip from the beamline optics. The

shoulder at 286.7 eV, relatively prominent for D1 corresponding to the contribution from π^* (C–OH) and π^* (C–O–C) transitions. The control sample shows negligible presence of aliphatic carbon (C–H) species, peak at 287.7 eV. For D1 instead, there is significant presence of aliphatic carbon at the surface. Thus, the respective decrease and increase in intensity of peaks at 285.5 eV and 287.7 eV can be related to the breaking of C=C bonds to form C–OH, aliphatic C–H & C–O–C species at the surface. While for D2 this effect is visible but not significant though. The intense peak at 288.5 eV for the untreated bacteria arise from the π^* (C=O) transitions and can be from either –COOH or –CONH₂ moieties. Studies by Gordon *et. al.* on inner shell excitation spectroscopy of the peptide bonds and proteins revealed that the π^* (C=O) transitions occurs between 288.2 and 288.6 eV. For D2 a shift of 0.2eV is observed for π^* (C=O) transitions while for D1 the shift increases to 0.4 eV relative to the control sample. This red shift can be attributed to the increase in electronegativity of the carbonyl core induced by neighboring atoms as reported by Urquhart and Ade.²⁰ Edwards and Myneni also reported the same in their NEXAFS studies of bacterial hydroxamate siderophores in aqueous solutions.²¹ The peak at 289.4 eV for the control sample could be due to various functional groups. As C–H and O-alkyl C groups in polysaccharides/carboxylic acids or CNH σ^* all have transitions at this energy value.^{22,23} The broad peak in the region of 291- 295 eV for all the samples comprises of multiple σ^* transitions, e.g C–N in amino acids (291 eV)²⁴ and C–O in alcohols and carboxylic acids (292.5 eV).^{25,26} A small peak at 297.5 eV for D2 is likely due to σ^* C–OH transitions. The broad peak around 304 eV for untreated bacteria corresponds to σ^* C=C transitions. In accordance to the π^* C=C transitions this σ^* transitions are suppressed for D1. Its worthy to mention that for D2 the spectral signature of various carbon moieties varied at different areas of the substrate. The uniformity of plasma func-

tionalization also depends on the extent of exposure. When the fan being on, the duration of interaction of the bacteria with plasma is non uniform with respect to the fan off condition. In the fan off state the bacteria have an extended interaction with the plasma, resulting in consistent spectral signature throughout the substrate.

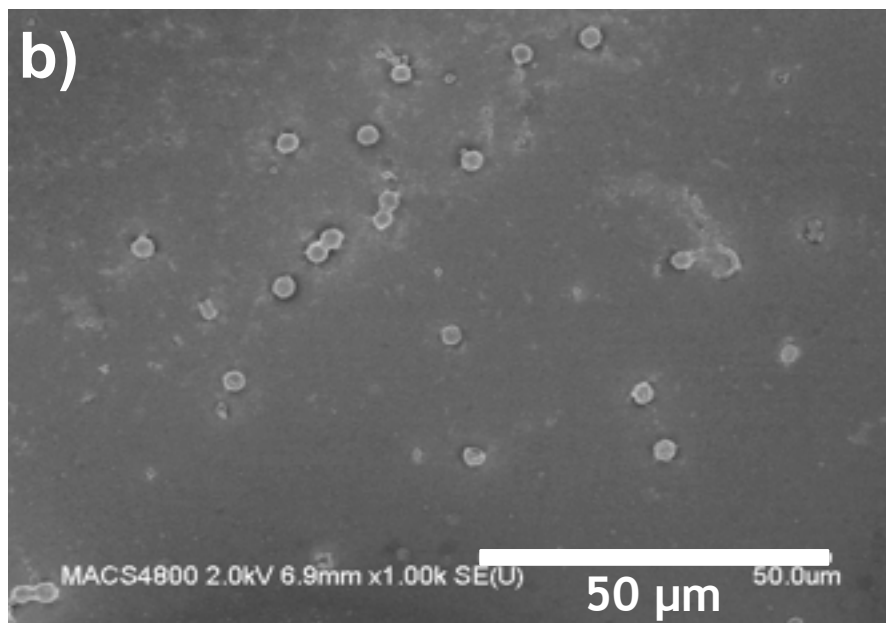
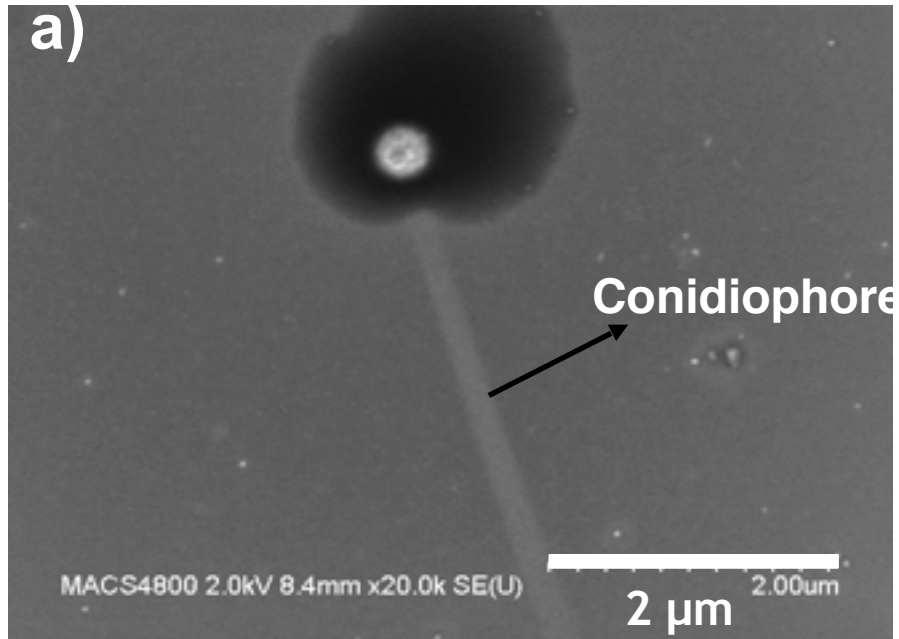
The O1s spectra for control sample exhibit an intense peak at 531.6 eV corresponding to π^* transitions of oxygen double bond moieties, which is considerably smaller for all other samples (D2>D1). According to Gordon *et al.* this peak can be attributed to O1s to π^* transitions of C=O groups of COOH and CONH₂ functionalities. Both C1s and O1s spectra indicate to the decreased concentration of C=O groups with respect to the control sample. The untreated sample shows a broad peak around 536 to 540 eV. Which can be due to contributions from multiple transitions comprising of Rydberg transitions, σ^* O–H and σ^* C–O transitions.^{22,25,27} For samples D1, D2 this broad peak can be clearly resolved into two peaks centered around 537 eV and 539 eV. According to previous report by Mangado *et al.* this peaks can be designated to σ^* O–H and σ^* C–O transitions respectively.¹⁴

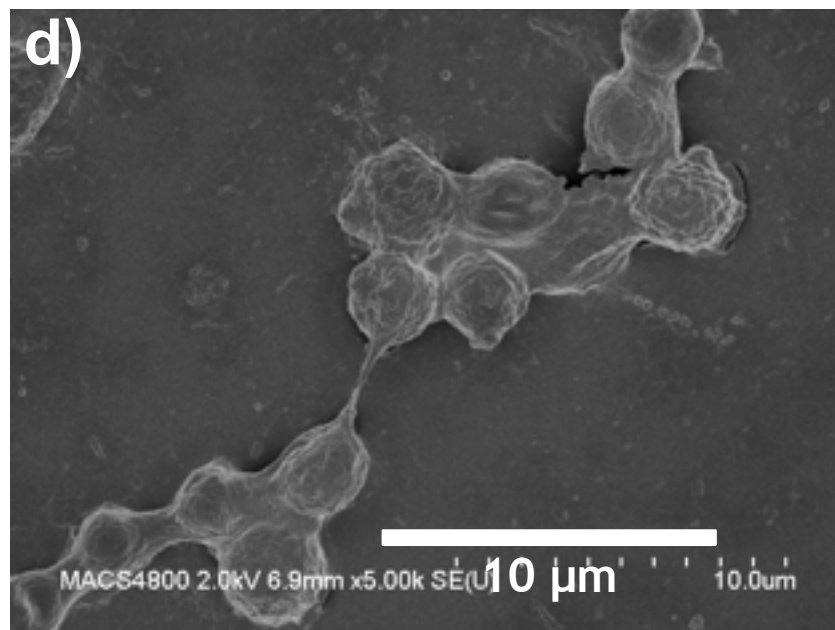
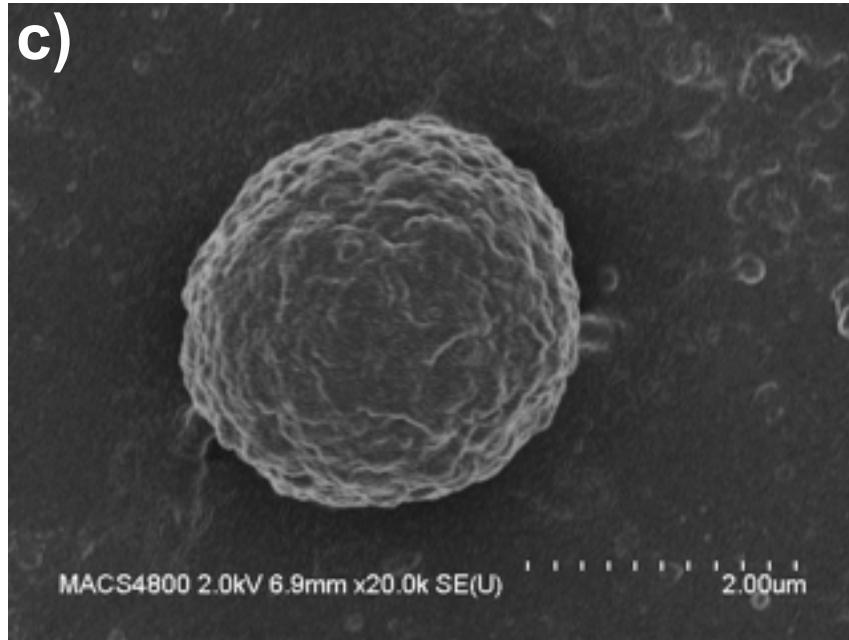
Figure 11(c) depicts variations in N Kedge spectra between the three samples. A low intensity peak at 398.7 eV corresponds to N1s to π^* (N=C) transitions. The intense peak at 401.2 eV can be related to the electronic transitions of $\pi^*_{(C=O)NH}$ of amide group. The decrease in intensity of this peak is consistent with the C1s and O1s spectra. Where a reduced concentration of C=O functional groups have also been observed. The peak around 405 eV is sharper for D1 and D2 with respect to the untreated sample. For the untreated sample this broad peak can be origination from multiple transitions including π^*_{N-O} , σ^*_{N-C} and Rydberg transitions.^{22,28} The sharpening of this peak for D1 and D2 is likely due to the increased concentration of nitro groups at the

surface of the bacteria. The broad peak around 412 eV can be designated to the σ^* (N=C) transitions in accordance to the reported value of Shard *et al.*²⁹ For D1 and D2 another peak can be observed at 416 eV which is absent for untreated bacteria is possibly due to σ^* (N=O) transitions. Although it is hard to deny the contribution of contaminants from the substrate and from ambient exposure. However, it is evident from the data shown in this plots that with the exposure to plasma the chemical functionalities at the surface of bacteria can be changed.

5. Deactivation of *Aspergillus Niger* (Fungi)

Before DBD treatment





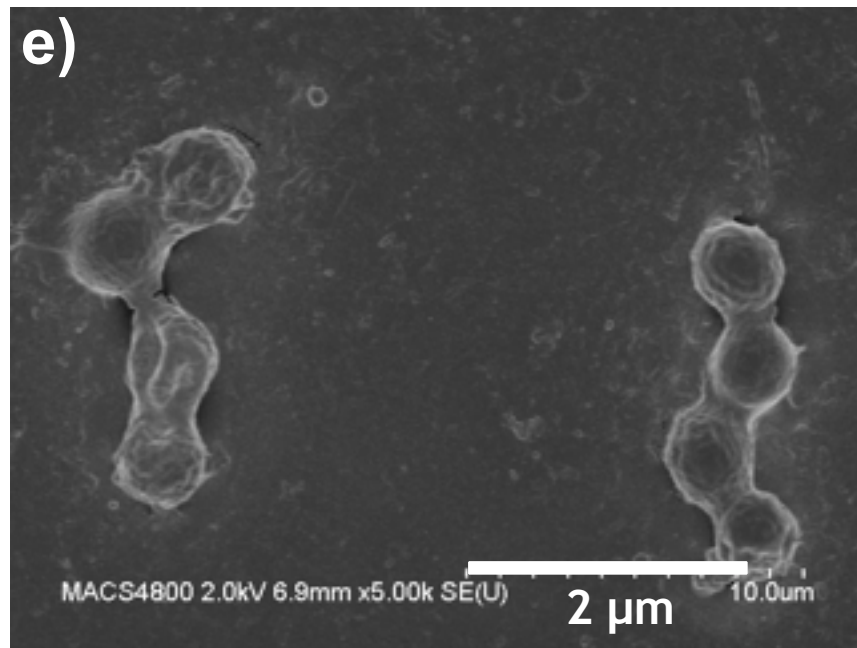
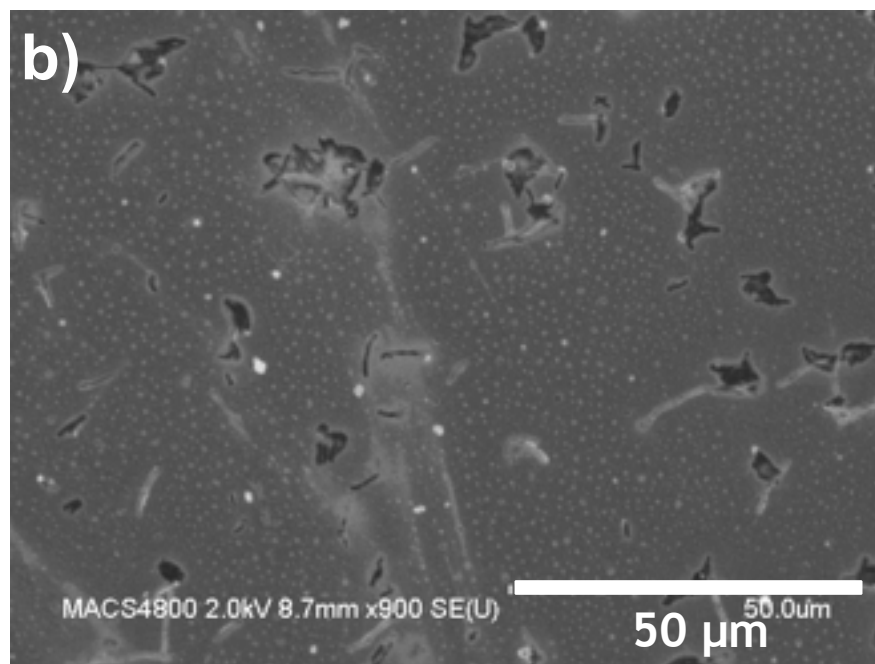
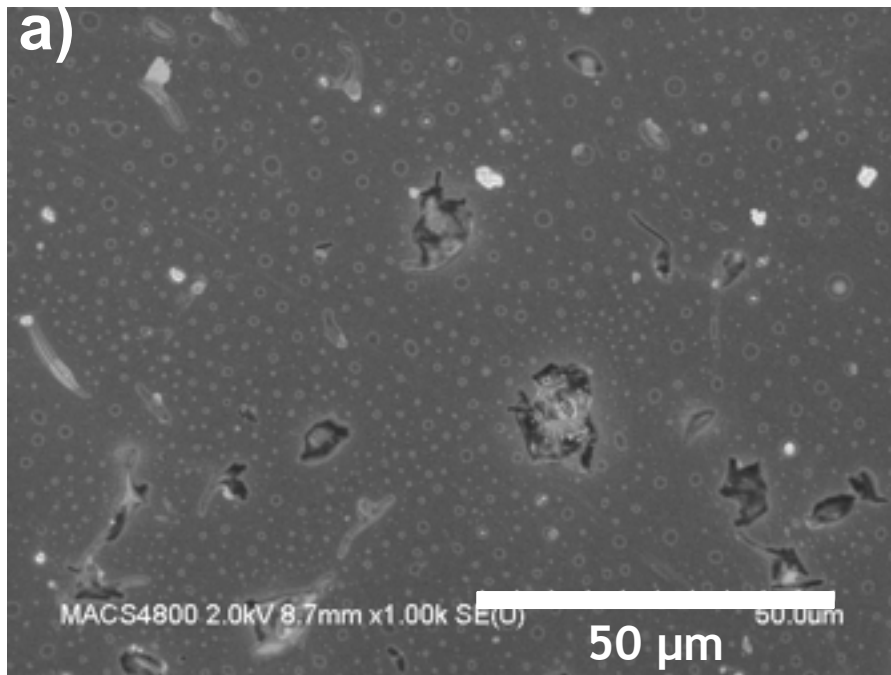
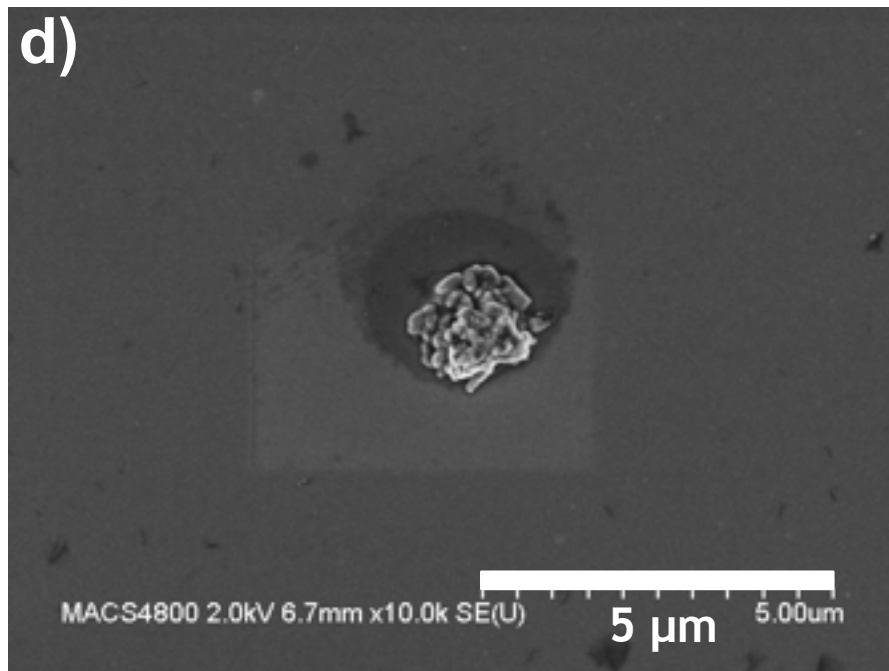
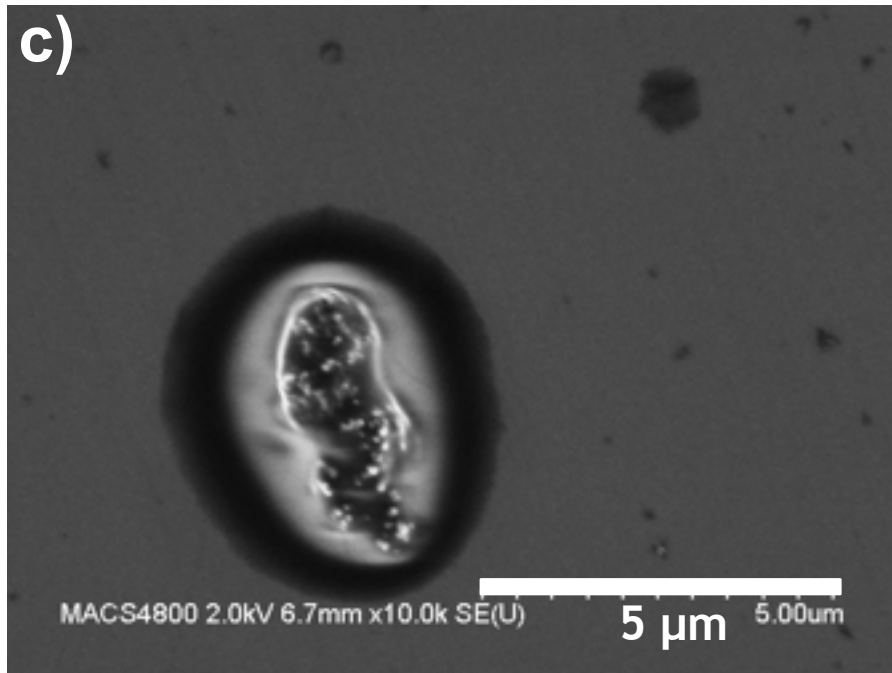


Figure 12. SEM images of aerosolised *Aspergillus Niger* Fungi

After DBD treatment:





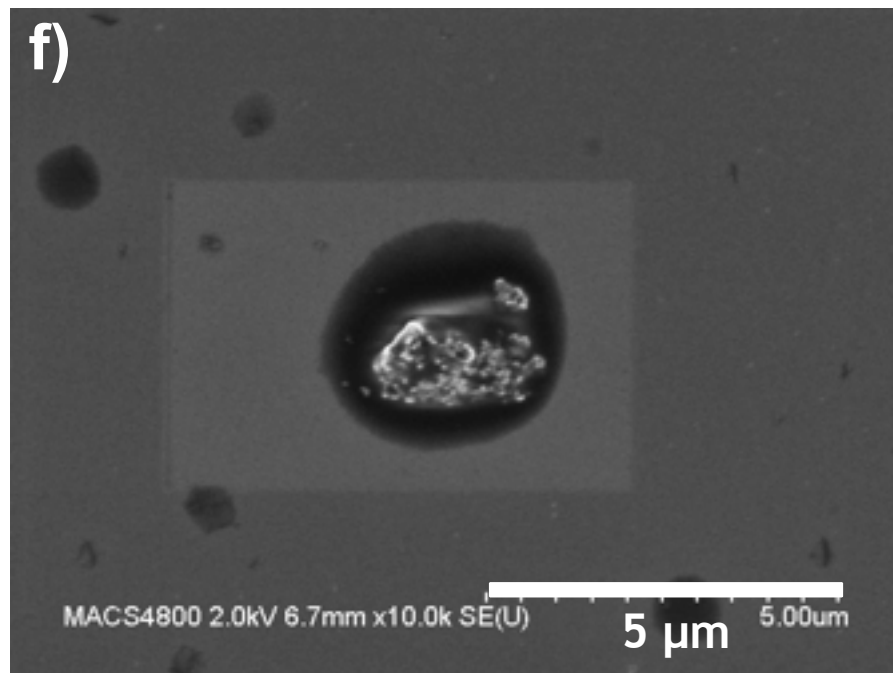
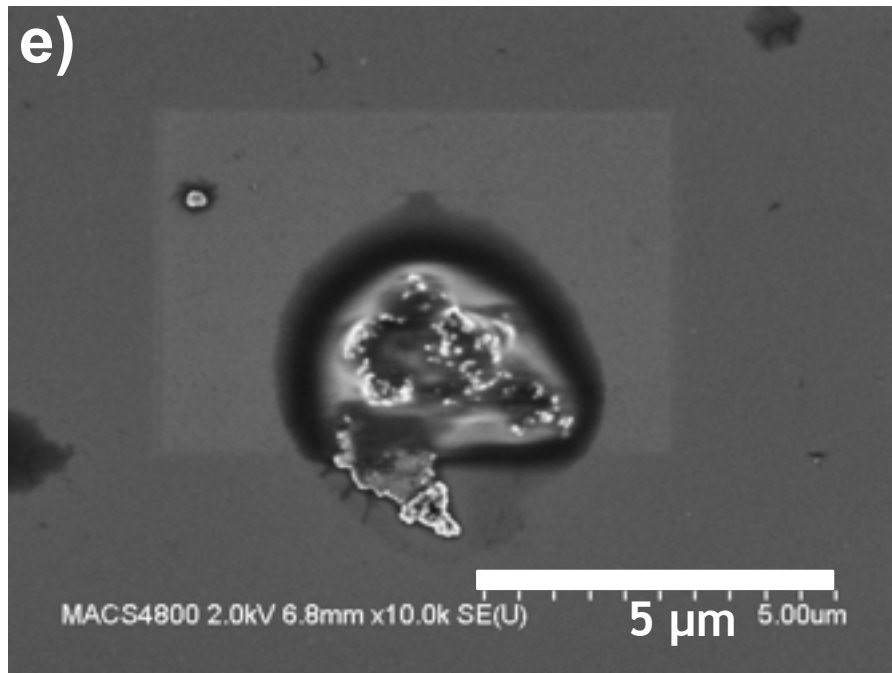


Figure 13. SEM images of DBD treated *Aspergillus Niger* Fungi

Airborne fungal spores can cause allergies as well as serious hospital-acquired infections. *Aspergillus niger* is one of the most common groups of fungi, and causes problems related to food industry and medicine, which makes it a suitable candidate for this study. Chitosan, a polysaccharide known for its anti-fungal activity would cause molecular disorganization and structural alterations of the cytoplasm and plasma membrane[30,31]. Plascencia-Jatomea et al., carried out the effect of temperature chitosan and temperature on *Aspergillus niger* and reported morphological changes of the spore upon treatment with chitosan [32].

Size and shape are important indices of cell envelope integrity. The SEM images clearly indicate morphological deformation in size and shape of the bacteria sustained by the cell envelope. Figures 12a to 12e shows SEM images of the *aspergillum niger* aerosolized and captured on a silicon substrate for fixing and imaging. It is evident from figures 12 a to 12c images that the spores were spherical in shape and figures 12d, 12e indicates that the spores were clumped, probably indicating polarity[32]. Figure 12a shows the fungus with conidiophore present at a imaging resolution of 2 micrometers.

Figures 13 a to 13f correspond to SEM images of aerosolized fungus, passed through DBD and captured on a silicon substrate for fixing and imaging. The morphological anomalies were evident in these DBD treated fungus. DBD treated fungus Figures 13a and 13b with 50 micrometer imaging resolution was compared to figure 12b untreated fungus. It is evident from these figures that the spores were echinulate. A similar observation was made by Plascencia-Jatomea et al., in

their work on chitosan based anti-fungal activity and attributed the echinulate spore formation to chitosan affected swelling. High resolution images (Figures 13c to 13f) of DBD treated fungus were compared with that of untreated fungus in Figures 12c to 12e and it is evident that the cell envelope integrity is broken upon DBD treatment. Reduction in size and severe distortion of the DBD treated spores indicate possible structural damage of the cell envelope, and leakage of cellular contents resulting in breakage of spores

6. CONCLUSIONS

In this work, we explored the efficacy of the atmospheric pressure dielectric barrier discharge (DBD) technology for inactivating airborne staphylococcus epidermidis. A systematic study was carried out to understand the effect of DBD on the morphology of *S. epidermidis* and *A.niger*. The aerosolized bacterial samples were collected from air in the vicinity of DBD and was analyzed for surface chemical change and morphological change upon DBD treatment. The scanning electron microscopic imaging of the *S. epidermidis* shows that the bacteria undergoes physical distortion to varying degrees resulting in loss of cellular materials. SEM images shows that *S. epidermidis* retains its shape, size and morphology when aerosolized and collected on a silicon wafer. Topographical changes in the structure of the bacteria were observed after treatment with DBD atmospheric plasma. From the SEM images it is concluded that the DBD causes severe size and shape change of the cell structure possibly resulting in destruction of cellular components and eventually to cell death. A similar effect was also found on the fungal spores. Thus indicating the versatility of the equipment toward a range of microorganisms.

7. REFERENCES:

1. Ziebuhr, W. *et al.* Nosocomial infections by *Staphylococcus epidermidis*: how a commensal bacterium turns into a pathogen. *Int. J. Antimicrob. Agents* **28 Suppl 1**, S14-20 (2006).
2. Cheung, G. Y. C. *et al.* *Staphylococcus epidermidis* strategies to avoid killing by human neutrophils. *PLoS Pathog.* **6**, e1001133 (2010).
3. Otto, M. *Staphylococcus epidermidis*--the 'accidental' pathogen. *Nat. Rev. Microbiol.* **7**, 555–67 (2009).
4. Otto, M. Staphylococcal biofilms. *Curr. Top. Microbiol. Immunol.* **322**, 207–28 (2008).
5. Costerton, J. W., Stewart, P. S. & Greenberg, E. P. Bacterial biofilms: a common cause of persistent infections. *Science* **284**, 1318–22 (1999).
6. Vuong, C. & Otto, M. *Staphylococcus epidermidis* infections. *Microbes Infect.* **4**, 481–9 (2002).
7. Domingo, P. & Fontanet, A. Management of complications associated with totally implantable ports in patients with AIDS. *AIDS Patient Care STDS* **15**, 7–13 (2001).
8. Ziebuhr, W. *Staphylococcus aureus* and *Staphylococcus epidermidis*: emerging pathogens in nosocomial infections. *Contrib. Microbiol.* **8**, 102–7 (2001).
9. Fridman, G. *et al.* Applied Plasma Medicine. *Plasma Process. Polym.* **5**, 503–533 (2008).
10. Morfill, G. E. *et al.* FOCUS ON PLASMA MEDICINE. *New J. Phys.* **11**, 115011 (2009).
11. Hee Lee, M. *et al.* Removal and sterilization of biofilms and planktonic bacteria by mi-

- crowave-induced argon plasma at atmospheric pressure. *New J. Phys.* **11**, 115022 (2009).
12. Weltmann, K. D. *et al.* Atmospheric-pressure plasma sources: Prospective tools for plasma medicine. *Pure Appl. Chem.* **82**, 1223–1237 (2010).
 13. Kong, M. G. *et al.* Plasma medicine: an introductory review. *New J. Phys.* **11**, 115012 (2009).
 14. Romero-Mangado, J. *et al.* Morphological and chemical changes of aerosolized E. coli treated with a dielectric barrier discharge. *Biointerphases* **11**, 11009 (2016).
 15. Laroussi, M. Low Temperature Plasma-Based Sterilization: Overview and State-of-the-Art. *Plasma Process. Polym.* **2**, 391–400 (2005).
 16. Daeschlein, G. *et al.* Antibacterial Activity of an Atmospheric Pressure Plasma Jet Against Relevant Wound Pathogens in vitro on a Simulated Wound Environment. *Plasma Process. Polym.* **7**, 224–230 (2010).
 17. Laroussi, M. Low-Temperature Plasmas for Medicine? *IEEE Trans. Plasma Sci.* **37**, 714–725 (2009).
 18. Matthes, R. *et al.* Antimicrobial Efficacy of an Atmospheric Pressure Plasma Jet Against Biofilms of *Pseudomonas aeruginosa* and *Staphylococcus epidermidis*. *Plasma Process. Polym.* **10**, 161–166 (2013).
 19. Tirsell, K. G. & Karpenko, V. P. A general purpose sub-keV X-ray facility at the Stanford Synchrotron Radiation Laboratory. *Nucl. Inst. Methods Phys. Res. A* **291**, 511–517 (1990).
 20. Urquhart, S. G. & Ade, H. Trends in the carbonyl core (C 1S, O 1S) $\pi^*c=o$ transition in the near-edge X-ray absorption fine structure spectra of organic molecules. *J. Phys. Chem. B* **106**, 8531–8538 (2002).

21. Edwards, D. C. & Myneni, S. C. B. Near edge X-ray absorption fine structure spectroscopy of bacterial hydroxamate siderophores in aqueous solutions. *J. Phys. Chem. A* **110**, 11809–18 (2006).
22. Gordon, M. L. *et al.* Inner-shell excitation spectroscopy of the peptide bond: Comparison of the C 1s, N 1s, and O 1s spectra of glycine, glycyl-glycine, and glycyl-glycyl-glycine. *J. Phys. Chem. A* **107**, 6144–6159 (2003).
23. Solomon, D., Lehmann, J., Kinyangi, J., Liang, B. & Schafer, T. Carbon K-Edge NEXAFS and FTIR-ATR Spectroscopic Investigation of Organic Carbon Speciation in Soils. *Soil Sci. Soc. Am. J.* **69**, 107–119 (2005).
24. Kaznatcheyev, K. *et al.* Innershell absorption spectroscopy of amino acids. *J. Phys. Chem. A* **106**, 3153–3168 (2002).
25. Outka, D. A. *et al.* NEXAFS studies of complex alcohols and carboxylic acids on the Si(111)(7×7) surface. *Surf. Sci.* **185**, 53–74 (1987).
26. Sette, F., Stöhr, J. & Hitchcock, A. P. Determination of intramolecular bond lengths in gas phase molecules from K shell shape resonances. *J. Chem. Phys.* **81**, 4906 (1984).
27. Stewart-Ornstein, J. *et al.* Using Intrinsic X-ray Absorption Spectral Differences To Identify and Map Peptides and Proteins. *J. Phys. Chem. B* **111**, 7691–7699 (2007).
28. Vairavamurthy, A. & Wang, S. Organic Nitrogen in Geomacromolecules: Insights on Speciation and Transformation with K-edge XANES Spectroscopy. *Environ. Sci. Technol.* **36**, 3050–3056 (2002).
29. Shard, A. G. *et al.* A NEXAFS Examination of Unsaturation in Plasma Polymers of Allylamine and Propylamine. *J. Phys. Chem. B* **108**, 12472–12480 (2004).

30. Zhang, D., Quantick, P. C., Antifungal effects of chitosan coating on fresh strawberries and raspberries during storage. *J. Hort. Sci. Biotech.* **73**, 763, (1998).
31. Roller, S., Covill, N., The antifungal properties of chitosan in laboratory media and apple juice. *Int. J. Food Microbiol.* **47**, 67, (1999).
32. Plascencia-Jatomea, M., Vinegar, G., Olayo, R., Castillo-Ortega, M.M., Shirai, K., Effect of Chitosan and Temperature on Spore Germination of *Aspergillus Niger*. *Macromol. Biosci.* **3**, 582, (2003).